

Journal of Mathematical Sciences and Modelling

JOURNAL OF MATHEMATICAL SCIENCES AND MODELLING

ISSN (Online) 2636-8692 https://dergipark.org.tr/en/pub/jmsm

Research Article

Tumor-Immune Dynamics: A Spatial-Spectral Perspective

Serpil Yılmaz [®]

Department of Computer Engineering, Faculty of Engineering and Architecture, İzmir Katip Çelebi University, İzmir, Türkiye 🗪

Article Info

Keywords: Basins of attraction, Dynamical systems, Entropy measures, Spectral analysis, Tumor-immune interactions

2020 AMS: 34C60, 37G35, 37N30,

65PXX, 92B05

Received: 21 April 2025 Accepted: 24 June 2025 Available online: 25 June 2025

Abstract

Mathematical modeling of tumor–immune interactions provides valuable insights into the nonlinear dynamics that govern tumor progression and response to treatment. In this study, a deterministic model of the tumor–immune system under chemotherapy is investigated with a focus on spectral entropy and basin of attraction analyses. Spectral entropy is applied to quantify the temporal complexity of system dynamics and to detect transitions between qualitatively distinct behavioral regimes, such as steady states, oscillatory patterns, and potentially chaotic trajectories. Basin of attraction analysis investigates how variations in the initial populations of tumor and immune cells determine the long-term behavior of the system, including tumor elimination, persistent oscillations, or uncontrolled tumor growth. By combining spectral entropy with basin mapping, the framework captures both the temporal irregularity and the sensitivity to initial conditions inherent in tumor–immune dynamics, which may help guide the design and timing of more effective therapeutic interventions.

1. Introduction

The use of mathematical models has become an essential interdisciplinary tool in cancer research, bridging mathematics, biology, and medicine to enhance understanding of cancer initiation, progression, and treatment. These models provide a structured framework for simulating complex biological processes, such as immune system activation and suppression. They also help identify the key factors of tumor behavior, whether it is eliminated, remains dormant, or grows uncontrollably. By adjusting model parameters, researchers can evaluate how treatment timing, dosage, and immune status influence therapeutic outcomes.

A wide range of models has been developed to study tumor–immune interactions. One foundational contribution by Kuznetsov et al. [1] introduced a nonlinear tumor–immune model, using parameter estimation and bifurcation analysis to determine the conditions for tumor elimination or persistence. Subsequent studies expanded these deterministic models [2–6]. Bifurcation analysis has also been used to explore the effects of immune system strength and pulsed therapy on tumor dynamics [7]. To capture the nonlinear and often unpredictable behavior of tumor growth, discrete and chaotic models have been proposed. A discrete map-based model demonstrated that tumor growth can transition between exponential, periodic, and chaotic patterns depending on parameter values [8]. A chaotic differential equation model demonstrated that variations in nutrient levels, such as glucose and oxygen, significantly influence tumor proliferation [9].

Time-delay effects have also been systematically investigated in mathematical oncology [10–13]. These models revealed oscillatory and chaotic behaviors that offer further insights into tumor relapse and immune regulation.

Mathematical modeling has also played a key role in the development of therapeutic strategies involving immunotherapy, chemotherapy, and their combinations [14–16]. Optimal control frameworks have been employed to develop effective treatment strategies, including immunotherapy and dendritic cell vaccination [17–19]. The efficiency of various combined treatments involving chemotherapy and radiotherapy has also been explored through mathematical modeling. These studies have examined how treatment intensity influences tumor dynamics and transitions to chaotic behavior [20–22]. Additionally, models that incorporate immunotherapy have been developed to investigate tumor oscillations and the potential for long-term relapse [23].

Recent advances in tumor-immune modeling include the integration of stochastic effects, spatial heterogeneity, and advanced control techniques. Stochastic models have demonstrated that random environmental fluctuations can significantly influence tumor progression and treatment efficacy [24]. The incorporation of the Allee effect in both deterministic and stochastic frameworks has provided valuable insights



into tumor extinction dynamics [25, 26]. Spatiotemporal models, which capture the spatial distribution and interaction of tumor and immune cells, have provided important insights into glioma control through immunotherapy [27, 28].

Additional efforts have focused on stabilizing chaotic tumor dynamics. A non-feedback control method has been proposed to regulate chaotic tumor behavior [29], while suboptimal dosing strategies have been shown to sustain chaos and delay tumor elimination [30]. Stochastic modeling has revealed that small perturbations can dramatically impact tumor outcomes [31–34]. Additionally, external interventions such as ultrasound and oncotripsy have been explored as potential tools to modulate chaos and enhance treatment effectiveness [35,36].

The complex interplay between tumor dynamics and the immune response during chemotherapy is inherently nonlinear and highly sensitive to both initial biological conditions and treatment parameters. Accurately characterizing these dynamics is essential for evaluating treatment efficacy and developing optimized therapeutic strategies.

In this study, spectral entropy (SE) is proposed as a diagnostic tool to analyze tumor–immune dynamics from both temporal and spatial perspectives. Spectral entropy quantifies the unpredictability of a time-series signal and is computed as the Shannon entropy of its normalized power spectral density (PSD) [37]. As a measure of temporal complexity, SE values indicate the degree of disorder in the system. Low SE reflects stable, predictable behavior, while high SE indicates irregular or oscillatory dynamics, potentially corresponding to unstable tumor–immune interactions or treatment resistance.

SE has been widely applied across various scientific domains. In biomedical signal processing, it has been used to detect state transitions and anomalies in EEG signals [38]. In speech processing, SE has applications in speaker identification and speech recognition [39–41], while in mechanical systems, it enables early fault detection by identifying subtle changes in vibration patterns [42]. These diverse applications highlight spectral entropy's capability to analyze complex and unpredictable behaviors; however, its application to tumor–immune modeling remains relatively unexplored.

To advance the analysis of tumor–immune interactions, spectral entropy is integrated with basin of attraction analysis to develop a spatial–spectral framework for exploring tumor–immune responses under varying chemotherapy intensities and initial conditions. Basin of attraction analysis reveals the system's long-term behavior by identifying how different initial conditions converge to distinct outcomes, such as tumor elimination, persistent oscillations characterized by recurring tumor growth and immune response, or uncontrolled growth.

Numerical simulations are conducted to assess the sensitivity of spectral entropy to variations in system parameters and initial states. This integrated spatial–spectral approach provides novel insights into the interplay between temporal and spatial dynamics in tumor–immune systems and highlights the potential of spectral entropy as a tool for optimizing chemotherapy strategies.

2. Tumor-Immune Model

In this study, we consider a deterministic model proposed in [20], which extends the model developed in [1] by incorporating an additional term to represent the effects of chemotherapy. This model describes the interactions between immune effector cells and tumor cells. The system is formulated as the following set of ordinary differential equations:

$$\dot{x} = \sigma + \rho \frac{xz}{\eta + z} - \mu xz - \delta x$$

$$\dot{z} = \alpha z (1 - \beta z) - xz - \frac{bz}{1 + z}$$
(2.1)

where x represents the population density of immune effector cells, and z denotes the population density of tumor cells. The term $-\frac{bz}{1+z^2}$ describes the effects of chemotherapy, where b represents the maximum efficacy of the drug. The parameter σ represents the natural rate of effector cell production in the tumor environment. The nonlinear term $\rho \frac{xz}{\eta+z}$ models immune stimulation due to tumor antigens, where ρ and η are parameters associated with tumor-specific antigens. The parameter μ characterizes the rate at which tumor cells inactivate effector cells, and δ is the natural death rate of effector cells.

To better illustrate the important characteristics of the quantitative dynamics of tumor cell density, a rescaling $z = y^4$ is applied to the system (2.1), as previously introduced in [31]. In terms of the variables x and y, the system (2.1) can be reformulated as:

$$\dot{x} = \sigma + \rho \frac{xy^4}{\eta + y^4} - \mu xy^4 - \delta x
\dot{y} = 0.25 \left(\alpha y (1 - \beta y^4) - xy - \frac{by}{1 + y^4} \right).$$
(2.2)

The parameter values used in this study are based on experimental data and previous modeling efforts presented in [1]:

$$\sigma = 0.1181, \quad \rho = 1.131, \quad \eta = 20.19, \quad \mu = 0.001, \quad \delta = 0.374 \quad \alpha = 1.636, \quad \beta = 0.002.$$
 (2.3)

The tumor-free equilibrium of the system corresponds to the point $(\bar{x}, \bar{y}) = (\frac{\sigma}{\delta}, 0)$. Linearization about this point yields the Jacobian matrix, whose eigenvalues are given by:

$$\lambda_1 = -\delta, \qquad \lambda_2 = 0.25 \left(\alpha - \frac{\sigma}{\delta} - b\right).$$

The first eigenvalue λ_1 is always negative, indicating stability in the *x*-direction. The second eigenvalue λ_2 governs stability in the tumor cell population. In the absence of chemotherapy (b=0), the tumor-free state is stable if the tumor growth rate satisfies $\alpha < \frac{\sigma}{\delta}$. However, when $\alpha > \frac{\sigma}{\delta}$, stability requires a sufficiently large treatment intensity. Specifically, the tumor-free equilibrium is locally asymptotically stable if:

$$b > b_* = \alpha - \frac{\sigma}{\delta} \tag{2.4}$$

where b_* denotes the minimum chemotherapy threshold required to stabilize the tumor-free equilibrium.

As noted in [31], the condition in (2.4) does not guarantee global tumor elimination. Nonlinear systems can exhibit multiple attractors, such as tumor persistence and tumor-free states, with basins of attraction that depend strongly on initial conditions. In such cases, a treatment strategy that is effective for one set of initial conditions may prove ineffective for another.

3. Spectral Entropy

The spectral entropy (SE) of a time series x(n), where n = 0, 1, 2, ..., N - 1, is computed as follows [37]: The signal is first mean-centered:

$$\tilde{x}(n) = x(n) - \frac{1}{N} \sum_{n=0}^{N-1} x(n)$$

where $\tilde{x}(n)$ denotes the mean-centered signal. The discrete Fourier transform (DFT) of $\tilde{x}(n)$ is computed as

$$X(k) = \sum_{n=0}^{N-1} x(n)e^{-j2\pi nk/N}, \quad k = 0, 1, 2, \dots, N-1.$$

where $j = \sqrt{-1}$ is the imaginary unit.

The one-sided power spectrum is then obtained by:

$$S(k) = \frac{|X(k)|^2}{N}, \quad k = 0, 1, 2, 3, \dots, \frac{N}{2} - 1.$$

The total spectral power is defined as

$$S_{\text{total}} = \sum_{k=0}^{\frac{N}{2}-1} S(k)$$

which is used to normalize the power spectrum and form a probability distribution p_k as:

$$p_k = \frac{S(k)}{S_{\text{total}}} = \frac{|X(k)|^2}{\sum_{k=0}^{\frac{N}{2}-1} |X(k)|^2}.$$

The spectral entropy is then computed using Shannon's entropy formula:

$$SE = -\sum_{k=0}^{\frac{N}{2}-1} p_k \ln p_k$$

and normalized spectral entropy is given by:

$$SE(N) = \frac{SE}{\ln\left(\frac{N}{2}\right)}. (3.1)$$

4. Simulation Results

In this section, the dynamical behavior of the tumor–immune model described by Equation (2.2) is investigated using the parameter values specified in Equation (2.3). The influence of the chemotherapy efficacy parameter b on the long-term dynamics is analyzed through the construction of a bifurcation diagram and phase portraits. The impact of initial conditions on the system's long-term behavior is examined using phase portraits, basins of attraction analysis, and spectral entropy (SE).

To construct the bifurcation diagram, the system governed by Equation (2.2) was numerically integrated using the initial conditions x(0) = 0.5 and y(0) = 0.5. For each value of the chemotherapy efficacy parameter b, the maximum values of the tumor population variable y were recorded and plotted, as shown in Figure 4.1. A total of 50,000 time series data points were used in the computation, with the first 10,000 points discarded to remove the transients.

As the chemotherapy efficacy parameter b is varied, the system exhibits three distinct dynamical regimes, as shown in Figure 4.1:

- For 0 < b < 0.9, the system settles into a stable equilibrium characterized by a high tumor burden. In this range, the chemotherapy intensity is insufficient to significantly reduce tumor growth, and the immune response fails to control the tumor population effectively.
- For $0.9 < b < b_*$, where $b_* = 1.329$, a pitchfork bifurcation occurs near b = 0.9. The system transitions from a steady state to periodic behavior in tumor dynamics, characterized by alternating phases of tumor reduction and regrowth. Such patterns may arise during treatment cycles that provide only temporary control over tumor progression without achieving long-term elimination.
- For $b > b_*$, the tumor population collapses to zero, and the system stabilizes at the tumor-free equilibrium $(\frac{\sigma}{\delta}, 0)$. In this case, the combined effects of chemotherapy and immune response are sufficient to eliminate the tumor from the system.

Phase portraits of system (2.2) were generated for various values of the chemotherapy efficacy parameter b, using fixed initial conditions x(0) = 0.5 and y(0) = 0.5, as shown in Figure 4.2. For small values of b, particularly when b < 0.9, trajectories converged to a high-tumor steady state. As b approached 0.9, the system transitioned to a limit cycle, indicating periodic oscillations in both tumor and immune cell populations. Biologically, the emergence of such periodic behavior reflects a recurrent pattern of tumor remission and relapse, where the immune system intermittently suppresses tumor progression, followed by tumor regrowth.

To further investigate the role of initial conditions, the system was analyzed at the critical value b = 0.9. Four distinct initial conditions were considered, and the corresponding phase trajectories are presented in Figure 4.3. The outcomes showed that the system could evolve toward either a high-tumor steady state or a limit cycle, depending on the initial state. This indicates the presence of multistability in the tumor–immune dynamics, where different long-term behaviors coexist under the same parameter value.

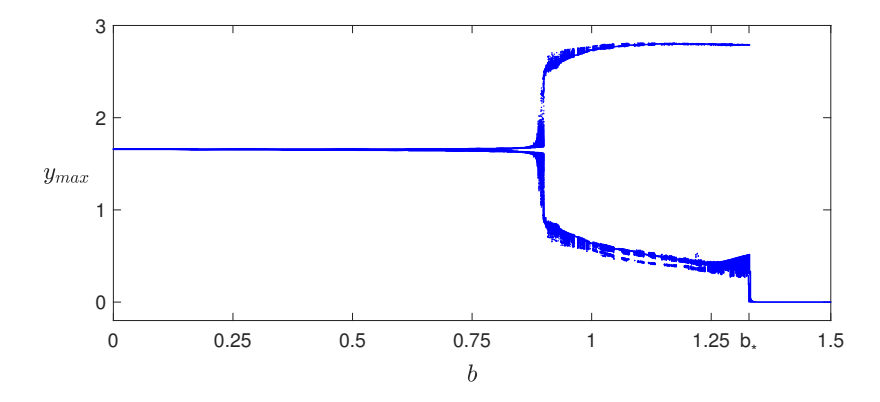
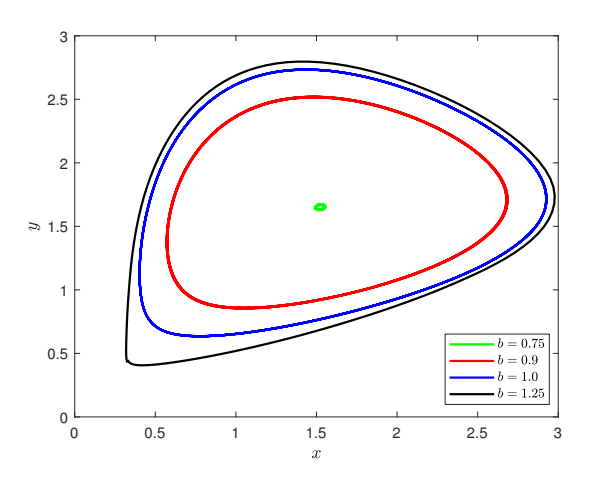


Figure 4.1: Bifurcation diagram of the tumor–immune system with respect to the chemotherapy efficacy parameter b, which represents the maximum effectiveness of the drug. The diagram shows the maximum values of the tumor population variable y as b increases, illustrating changes in the system's behavior. These changes highlight the sensitive dependence of tumor–immune interactions on the value of b.



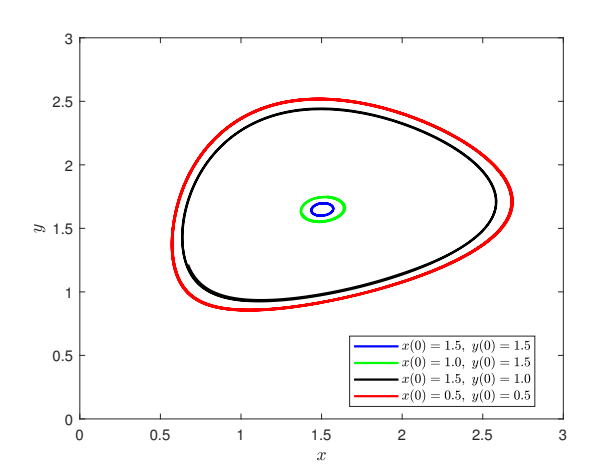


Figure 4.2: Phase portraits of system (2.2) for different values of the chemotherapy parameter b, with initial conditions x(0) = 0.5 and y(0) = 0.5. The trajectories illustrate the system's response to as b increases from 0.75 to 1.25. Increasing b affects the behavior of tumor—immune oscillations.

Figure 4.3: Phase portraits of system (2.2) at b=0.9, showing how different initial conditions affect long-term behavior. Each trajectory represents a different initial condition.

The spectral entropy (SE) of the system (2.2) was computed using Equation 3.1 as a function of b, for two different initial conditions: x(0) = 0.5, y(0) = 0.5 (red curve) and x(0) = 1.5, y(0) = 1.5 (blue curve), as shown in Figure 4.4. In comparison with the bifurcation diagram presented in Figure 4.1, the SE values remain low for b < 0.9, indicating steady-state behavior. A sharp increase in SE is observed near b = 0.9, indicating a transition to oscillatory or complex dynamics. For $b > b_* = 1.329$, SE values decrease again, reflecting a return to regular, tumor-free dynamics. The divergence between the red and blue curves highlights the system's sensitivity to initial conditions and demonstrates multistability in the tumor-immune interactions.

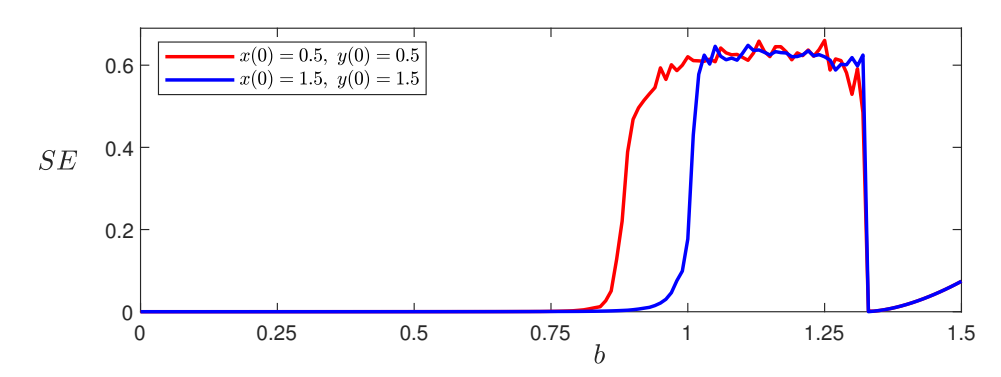


Figure 4.4: Spectral entropy (SE) as a function of the bifurcation parameter b, computed for two initial conditions: x(0) = 0.5, y(0) = 0.5 (red) and x(0) = 1.5, y(0) = 1.5 (blue). The SE quantifies the complexity of system dynamics as b varies. A sharp increase in SE indicates a transition to oscillatory or complex behavior. The figure highlights how this transition occurs at different values of b depending on initial conditions, demonstrating multistability in the system.

To examine the sensitivity of long-term dynamics to initial conditions, basins of attraction were computed over the domain x(0), $y(0) \in [0,3]$, using a 400×400 grid with evenly spaced values along each axis. This grid was utilized to explore a wide range of initial conditions and to capture the system's behavior across different regions of its phase space. The analysis was performed at a fixed value of the chemotherapy efficacy parameter b, selected to represent the critical transition period associated with bifurcations in system dynamics.

For each initial condition, the corresponding attractor was identified using a recurrence-based automated classification technique, as described in [43]. This method enables efficient classification of attractors without requiring detailed prior knowledge of the system's dynamics. The resulting classification map is shown in Figure 4.5, where each point represents an initial condition and is colored according to the type of attractor reached over time.

Two primary regions were identified within the state space:

- Purple Region: This region corresponds to a stable, steady state characterized by a high tumor burden. Initial conditions within this region lead to tumor persistence with minimal or no reduction. This indicates that chemotherapy is ineffective or the immune response is insufficient.
- *Gray Region:* This region is associated with oscillatory dynamics, where the system exhibits periodic limit cycle behavior. Tumor levels fluctuate between high and low states, reflecting a scenario in which the immune system intermittently suppresses tumor growth but fails to achieve complete elimination.

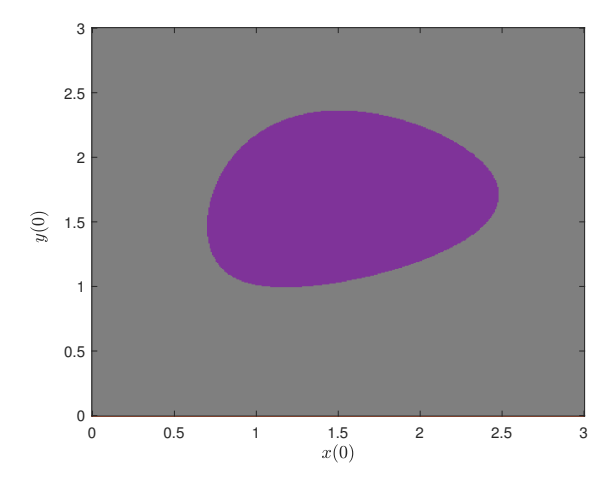


Figure 4.5: Basin of attraction of system (2.2) for initial conditions $x(0), y(0) \in [0,3]$, at a fixed parameter value of b. The purple region corresponds to trajectories converging to a stable steady state with high tumor burden, while the gray region represents initial conditions that lead to oscillatory dynamics associated with a limit cycle. The figure illustrates the coexistence of distinct long-term behaviors and shows that outcomes depend sensitively on initial conditions.

The basins of attraction shown in Figure 4.5 reveal sharply defined boundaries between dynamic regimes. This indicates high sensitivity to initial conditions. Even small changes in the initial tumor–immune states can lead to significantly different long-term behaviors. The presence of distinct attractor regions confirms that the system is multistable, which means that different therapeutic outcomes can occur depending on the initial tumor–immune conditions.

To further investigate the dynamical complexity within these regions, spectral entropy was computed for each trajectory across the grid of initial conditions. SE quantifies the unpredictability and complexity of the system's temporal behavior. Figure 4.6 presents the SE values over the same domain $x(0), y(0) \in [0,3]$, with each point corresponding to the SE value of a specific initial condition.

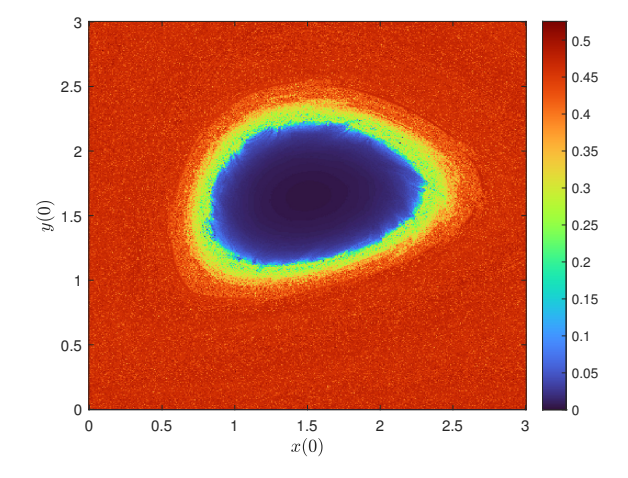


Figure 4.6: Spectral entropy of system (2.2) evaluated over the domain $x(0), y(0) \in [0,3]$ for a fixed value of b. Colors indicate the SE values, with dark blue representing regular (low-complexity) dynamics and red representing complex or chaotic oscillatory behavior. This figure provides a phase space map of dynamical complexity, illustrating how different initial conditions lead to qualitatively distinct temporal patterns in terms of entropy.

Low SE values, shown in dark blue in Figure 4.6, correspond to stable high-tumor states. These points predominantly appear within the purple region of the basin of attraction plot in Figure 4.5, where the system converges to a steady equilibrium with a persistently high tumor burden. Conversely, higher SE values, shown in warmer colors such as yellow and red, indicate more complex or oscillatory behavior. These values occur in the gray region of the basins of attraction in Figure 4.5, associated with limit cycle dynamics where tumor and immune cell populations fluctuate over time.

The SE map complements the basin of attraction diagram by revealing the degree of dynamical complexity in each region. While the basins of attraction illustrate the long-term outcomes, the SE map highlights areas exhibiting chaotic or complex transient dynamics. Notably, near the boundary between the purple and gray regions, small variations in initial conditions lead to significant changes in the final state, reflected by high SE values. This sensitivity suggests the presence of multiple possible therapeutic outcomes, even with slight differences in initial tumor and immune cell densities.

5. Conclusion

This study presented a spatial-spectral framework to analyze tumor-immune dynamics under chemotherapy by integrating basin of attraction mapping with spectral entropy analysis. Basin mapping revealed multistability, which shows that identical treatment parameters can lead to different outcomes depending on the initial tumor-immune conditions. A wider basin corresponding to a desirable state, such as low tumor burden, indicates a more robust therapeutic outcome and improved long-term tumor control. Spectral entropy provided a quantitative measure of temporal complexity and effectively highlighted regime transitions, with high values near bifurcations and along intricate basin boundaries. The combined approach identified regions highly sensitive to both treatment parameters and initial conditions. These findings offer valuable insights to guide the design of more predictable and effective treatment strategies.

Article Information

Acknowledgements: The author would like to express sincere thanks to the editor and the anonymous reviewers for their helpful comments and suggestions.

Artificial Intelligence Statement: No AI tools were used in the preparation of this manuscript.

Conflict of Interest Disclosure: No potential conflict of interest was declared by the author.

Plagiarism Statement: This article was scanned by the plagiarism program.

References

- [1] V. A. Kuznetsov, I. A. Makalkin, M. A. Taylor, et al., Nonlinear dynamics of immunogenic tumors: parameter estimation and global bifurcation analysis, Bull. Math. Biol., 56(2) (1994), 295-321. http://dx.doi.org/10.1007/BF0246064
- [2] L. G. de Pillis, W. Gu, A. E. Radunskaya, Mixed immunotherapy and chemotherapy of tumors: Modeling, applications and biological interpretations, J. Theoret. Biol., 238(4) (2006), 841–862. https://doi.org/10.1016/j.jtbi.2005.06.037
- [3] L. G. De Pillis, A. Radunskaya, The dynamics of an optimally controlled tumor model: A case study, Math. Comput. Modelling, 37(11) (2003),
- [4] A. d'Onofrio, A general framework for modeling tumor-immune system competition and immunotherapy: Mathematical analysis and biomedical inferences, Physica D: Nonlinear Phenom., 208(3-4) (2005), 220–235. https://doi.org/10.1016/j.physd.2005.06.032
- [5] D. Kirschner, J. C. Panetta, Modeling immunotherapy of the tumor-immune interaction, J. Math. Biol., 37 (1998), 235–252. https://doi.org/10.1007/
- [6] V. A. Kuznetsov, G. D. Knott, Modeling tumor regrowth and immunotherapy, Math. Comput. Modelling, 33(12-13) (2001), 1275–1287. https: //doi.org/10.1016/S0895-7177(00)00314-
- [7] H. C. Wei, J. T. Lin, Periodically pulsed immunotherapy in a mathematical model of tumor-immune interaction, Internat. J. Bifur. Chaos Appl. Sci. Engrg., 23(04) (2013), Article ID 1350068. https://doi.org/10.1142/S021812741350068
- M. Moghtadaei, M. R. H. Golpayegani, R. Malekzadeh, Periodic and chaotic dynamics in a map-based model of tumor-immune interaction, J. Theoret. Biol., 334 (2013), 130–140. https://doi.org/10.1016/j.jtbi.2013.05.031
- [9] M. Harney, W. S. Yim, Chaotic attractors in tumor growth and decay: a differential equation model, In: P. Vlamos, A. Alexiou (eds) GeNeDis 2014, Adv. Exp. Med. Biol., **820** (2014), Springer, Cham, 193–206. https://doi.org/10.1007/978-3-319-09012-2_13
- [10] D. Ghosh, S. Khajanchi, S. Mangiarotti, et al., How tumor growth can be influenced by delayed interactions between cancer cells and the microenvironment?, BioSystems, 158 (2017), 17-30. https://doi.org/10.1016/j.biosystems.2017.05.001 [11] X. E. Zhao, B. Hu, The impact of time delay in a tumor model, Nonlinear Anal.: Real World Appl., 51 (2020), Article ID 103015. https://doi.org/10.
- [12] S. Khajanchi, M. Perc, D. Ghosh, The influence of time delay in a chaotic cancer model, Chaos, 28(10) (2018), Article ID 103101. https://doi.org/10. M. Sardar, S. Khajanchi, S. Biswas, et al., A mathematical model for tumor-immune competitive system with multiple time delays, Chaos Solitons
- Fractals, **179** (2024), Article ID 114397. https://doi.org/10.1016/j.chaos.2023.114397 J. Yang, S. Tang, R. A. Cheke, Modelling pulsed immunotherapy of tumour-immune interaction, Math. Comput. Simulation, 109 (2015), 92–112.
- https://doi.org/10.1016/j.matcom.2014.09.001 [15] P. Das, S. Das, P. Das, et al., Optimal control strategy for cancer remission using combinatorial therapy: A mathematical model-based approach, Chaos
- Solitons Fractals, 145 (2021), Article ID 110789. https://doi.org/10.1016/j.chaos.2021.110789 C. Letellier, S. K. Sasmal, C. Draghi, et al., A chemotherapy combined with an anti-angiogenic drug applied to a cancer model including angiogenesis,
- Chaos Solitons Fractals, 99 (2017), 297-311. https://doi.org/10.1016/j.chaos.2017.04.013 M. Sardar, S. Biswas, S. Khajanchi, Modeling the dynamics of mixed immunotherapy and chemotherapy for the treatment of immunogenic tumor, Eur.
- Phys. J. Plus, 139(3) (2024), 1-26, Article ID 228. https://doi.org/10.1140/epjp/s13360-024-05004-6 [18] M. Sardar, S. Khajanchi, B. Ahmad, A tumor-immune interaction model with the effect of impulse therapy, Commun. Nonlinear Sci. Numer. Simul., 126
- (2023), Article ID 107430. https://doi.org/10.1016/j.cnsns.2023.107430 [19] S. Khajanchi, J. Mondal, P. K. Tiwari, Optimal treatment strategies using dendritic cell vaccination for a tumor model with parameter identifiability, J.
- Biol. Syst., 31(02) (2023), 487-516. https://doi.org/10.1142/S0218339023500171 I. Bashkirtseva, A. Chukhareva, L. Ryashko, Modeling and analysis of nonlinear tumor-immune interaction under chemotherapy and radiotherapy,
- Math. Methods Appl. Sci., **45**(13) (2022), 7983–7991. https://doi.org/10.1002/mma.7706 I. Bashkirtseva, L. Ryashko, A. G. López, et al., The effect of time ordering and concurrency in a mathematical model of chemoradiotherapy, Commun.
- Nonlinear Sci. Numer. Simul., 96 (2021), Article ID 105693. https://doi.org/10.1016/j.cnsns.2021.105693

- [22] I. Bashkirtseva, L. Ryashko, J. M. Seoane, et al., Chaotic transitions in a tumor-immune model under chemotherapy treatment, Commun. Nonlinear Sci. Numer. Simul., 132 (2024), Article ID 107946. https://doi.org/10.1016/j.cnsns.2024.107946
- G. Torres Espino, C. Vidal, Dynamics aspects and bifurcations of a tumor-immune system interaction under stationary immunotherapy, Math. Biosci., **369** (2024), Article ID 109145. https://doi.org/10.1016/j.mbs.2024.109145
- M. Sardar, S. Khajanchi, S. Biswas, Stochastic dynamics of a nonlinear tumor-immune competitive system, Nonlinear Dyn., 113 (2025), 4395-4423. https://doi.org/10.1007/s11071-024-09768-5
 [25] S. Khajanchi, M. Sardar, J. J. Nieto, Application of non-singular kernel in a tumor model with strong Allee effect, Differ. Equ. Dyn. Syst., 31(3) (2023),
- 687-692. https://doi.org/10.1007/s12591-022-00622-x
- M. Sardar, S. Khajanchi, Is the Allee effect relevant to stochastic cancer model?, J. Appl. Math. Comput., 68 (2022), 2293-2315. https://doi.org/10.1007/
- [27] S. Khajanchi, J. J. Nieto, Spatiotemporal dynamics of a glioma immune interaction model, Sci. Rep., 11 (2021), Article ID 22385. https://doi.org/10.
- S. Khajanchi, The impact of immunotherapy on a glioma immune interaction model, Chaos Solitons Fractals, 152 (2021), Article ID 111346. https://doi.org/10.1016/j.chaos.2021.111346
- S. Sabarathinam, K. Thamilmaran, Controlling of chaos in a tumour growth cancer model: An experimental study, Electron. Lett., 54(20) (2018),
- 1160–1162. https://doi.org/10.1049/el.2018.5126
 M. Saleem, M. Y. Baba, A. Raheem, et al., A caution for oncologists: Chemotherapy can cause chaotic dynamics, Comput. Methods Programs Biomed., 200 (2021), Article ID 105865. https://doi.org/10.1016/j.cmpb.2020.105865
- I. Bashkirtseva, A. Chukhareva, L. Ryashko, Stochastic dynamics of nonlinear tumor-immune system with chemotherapy, Phys. A: Stat. Mech. Appl., 622 (2023), Article ID 128835. https://doi.org/10.1016/j.physa.2023.128835
- [32] I. Bashkirtseva, L. Ryashko, Analysis of noise-induced phenomena in the nonlinear tumor-immune system, Phys. A, 549 (2020), Article ID 123923. https://doi.org/10.1016/j.physa.2019.123923
- [33] I. Bashkirtseva, L. Ryashko, J. Duarte, et al., The role of noise in the tumor dynamics under chemotherapy treatment, Eur. Phys. J. Plus, 136 (2021), -13, Article ID 1123. https://doi.org/10.1140/epjp/s13360-021-02061-z
- [34] X. Liu, Q. Li, J. Pan, A deterministic and stochastic model for the system dynamics of tumor-immune responses to chemotherapy, Phys. A: Stat. Mech. Appl., 500 (2018), 162–176. https://doi.org/10.1016/j.physa.2018.02.118
- S. Abernethy, R. J. Gooding, The importance of chaotic attractors in modelling tumour growth, Phys. A: Stat. Mech. Appl., 507 (2018), 268–277.
- https://doi.org/10.1016/j.physa.2018.05.093
 [36] S. Yılmaz, Stabilization of chaos in a cancer model: The effect of oncotripsy, Balkan J. Electr. Comput. Eng., 10(2) (2022), 139–149. https:
- //doi.org/10.17694/bajece.1039384
 [37] G. Powell, I. Percival, A spectral entropy method for distinguishing regular and irregular motion of Hamiltonian systems, J. Phys. A: Math. Gen., 12(11) 1979), Article ID 2053. https://doi.org/10.1088/0305-4470/12/11/017
- [38] H. Helakari, J. Kananen, N. Huotari, et.al, Spectral entropy indicates electrophysiological and hemodynamic changes in epilepsy, NeuroImage Clin., 22 (2019), Article ID 101763. https://doi.org/10.1016/j.nicl.2019.101763
- F. Luque-Suárez, A. Camarena-Ibarrola, E. Chávez, Efficient speaker identification using spectral entropy, Multimed. Tools Appl., 78 (2019),
- [40] A. M. Toh, R. Togneri, S. Nordholm, Spectral entropy as speech features for speech recognition, Proc. PEECS, 1 (2005), Article ID 92.
 [41] H. Misra, S. Ikbal, H. Bourlard, et al., Spectral entropy based feature for robust ASR, Proc. IEEE Int. Conf. Acoust. Speech Signal Process., 1 (2004), 1–193. https://doi.org/10.1109/ICASSP.2004.1325955
 [42] K. Wang, Z. J. Xu, Y. Gong, et al., Mechanical fault prognosis through spectral analysis of vibration signals, Algorithms, 15(3) (2022), Article ID 94.
- nttps://doi.org/10.3390/a15030094
- [43] G. Datseris, A. Wagemakers, Effortless estimation of basins of attraction, Chaos, 32(2) (2022), Article ID 023104. https://doi.org/10.1063/5.0076568